WIND-TUNNEL PRESSURE MEASUREMENTS ON MODEL-SCALE RIGID DOWNWIND SAILS

Patrick Bot, Naval Academy Research Institute, France, patrick.bot@ecole-navale.fr
Ignazio Maria Viola, Yacht and Superyacht Research Group, School of Marine Science and Technology, Newcastle University, UK, ignazio.viola@newcastle.ac.uk
Richard G.J. Flay, Yacht Research Unit, University of Auckland, New Zealand, r.flay@auckland.ac.nz
Jean-Sebastien Brett, Naval Academy Research Institute, France, jean-sebastien.brett@gadz.org

This paper describes an experiment that was carried out in the Twisted Flow Wind Tunnel at The University of Auckland to measure a detailed set of pressure distributions on a rigid 1/15th scale model of a modern asymmetric spinnaker. It was observed that the pressures varied considerably up the height of the spinnaker. The fine resolution of pressure taps allowed the extent of leading edge separation bubbles, pressure recovery region, and effect of sail curvature to be observed quite clearly. It was found that the shape of the pressure distributions could be understood in terms of conventional aerodynamic theory. The sail performed best at an apparent wind angle of about 55°, which is its design angle, and the effect of heel was more pronounced near the head than the foot.

NOMENCLATURE

AWA	Apparent Wind Angle (°)
AWA_{eff}	Effective Apparent Wind Angle (°)
c	Sail section chord (m)
c_{av}	Average sail chord (m)
$Cp = \frac{p-p_\infty}{q_\infty}$	Pressure coefficient (-)
f	Frequency (Hz)
h	Yacht model height (m)
p	Sail surface pressure (Pa)
p_∞	Reference static pressure (Pa)
q_∞	Reference dynamic pressure (Pa)
$Re = \frac{U_\infty h}{\nu}$	Reynolds number (-)
$St = \frac{fc}{U_\infty}$	Strouhal number (-)
U_∞	Reference velocity ($m \cdot s^{-1}$)
x	chord-wise coordinate (m)

1 INTRODUCTION

Modern yacht sails are aerodynamically very efficient but the flow field around sails is largely unknown. Knowledge of the flow features that make sails aerodynamically efficient will allow the performance of sails and also the aerodynamic efficiency of sail-like airfoils for other applications to be enhanced further.

The aerodynamics of sails has mainly been investigated with force measurements [1-5] in wind tunnels [6-8], while only a few authors have recently measured sail pressure distributions [9-11]. The flow field around sails has been examined primarily through numerical simulations and, therefore, it is very important to validate such simulations with accurate measurements of local quantities such as surface pressure distributions, instead of only comparing them to global quantities such as forces.

Sail pressure distributions can be measured in model-scale from wind tunnel tests and in full scale [11]. The state-of-the-art experimental technique is based on flexible sails – including semi-flexible single-skin fibreglass sails used by Richards and Lasher [9], and common spinnaker sailcloth used by Viola & Flay [10,12] - where pressure taps are attached to one side of the sail and pressures are measured on the other side of the sail through holes in the sailcloth. This technique allows realistic sail trims in different sailing conditions to be modelled, but is limited by (i) the unknown blockage effect due to the tubes and pressure taps, (ii) the alteration of both the static sail shape and the dynamic behaviour of the sails by the mass and stiffness of the tubes and pressure taps, (iii) the low accuracy in the reconstruction of the sail flying shape.

The observed differences between the pressure distributions measured with this technique in the wind tunnel, and those measured in full-scale or computed numerically are expected to be partially due to the presence of tubes and pressure taps.

A novel technique is presented in this paper, where the effect of the pressure taps is eliminated and the effect of the tubes on the flow field is minimised. Also, the sail is rigid allowing the flying shape to be detected with high-accuracy.

This paper describes pressure distributions measured on the rigid asymmetric spinnaker in a wind tunnel, which are discussed and compared to pressures measured on soft flexible sails, and also to numerical simulation results. The pressure profiles along the sail chord on the leeward side enable interesting flow characteristics to be determined, such as leading edge separation bubble (sharp suction peak), sail curvature suction, and trailing

edge flow separation (pressure plateau). Helpful insights into sail aerodynamics are obtained from this investigation, which are explained using conventional aerodynamic and aeronautical knowledge of the aerodynamics of thin wings. Further details are given in the subsequent sections.

2 EXPERIMENTAL ARRANGEMENT

A rigid 1/15th scale model of an AC33-class spinnaker has been tested at the University of Auckland Yacht Research Unit (YRU) Twisted Flow Wind Tunnel which has an open jet with a test section 7m wide and 3.5m high. The tests were performed in uniform flow (without twisting vanes) with a turbulence intensity of around 3%. The reference wind speed was approximately $U_\infty = 3.5\mathrm{m/s}$ giving a Reynolds number based on the average spinnaker chord c_{av} equal to $Re = 4 \cdot 10^5$. The solid spinnaker and mainsail were mounted on a yacht model (rig and hull), which was mounted on a turntable to adjust the apparent wind angle (AWA). The model was mounted on fore and aft bearings to enable the heel angle to be varied. Figure 1 shows two photographs of the model during the tests. In particular, Figure 1(b) shows the tubes carrying the pressures from the sail leech to the transducers in the cockpit; note also that the rig was reinforced by a deck spreader to windward due to the heavy spinnaker model, and the actuator used to adjust heel angle on the left hand side.

The solid model spinnaker was built as part of a master's research project at the YRU by Brett [13], with the flying shape recorded from a sailcloth model spinnaker previously studied at the YRU [10]. The selected shape was recorded for a trim giving the maximum driving force with a non-flapping sail at an AWA of 55° and 10° of heel. The geometric parameters of the sail shape are given in Table 1. Unfortunately the shapes of the rigid asymmetric spinnaker and the soft sail were not perfectly identical, and this has implications on the pressure comparisons discussed in Section 4.

The solid sail is a 5mm thick epoxy fibreglass sandwich where the core is a corrugated plastic material featuring a high density of individual pressure-tight flutes, which provide the pneumatic tubes to carry the pressure signal from the measurement location to the sail leech. Thin plastic tubes are connected to each flute on the sail leech to carry the pressure to the pressure transducers in the model cockpit. One-millimetre holes were drilled through the sail and tape was used to close one side in order to measure the pressures on the other side. A sketch of a pressure tap in section of the solid spinnaker model is shown in Figure 2. The rigid sail had a mass of about 10kg, and it was observed that its shape could distort due to self-weight. The implications of this are addressed later in the paper when the results are discussed.

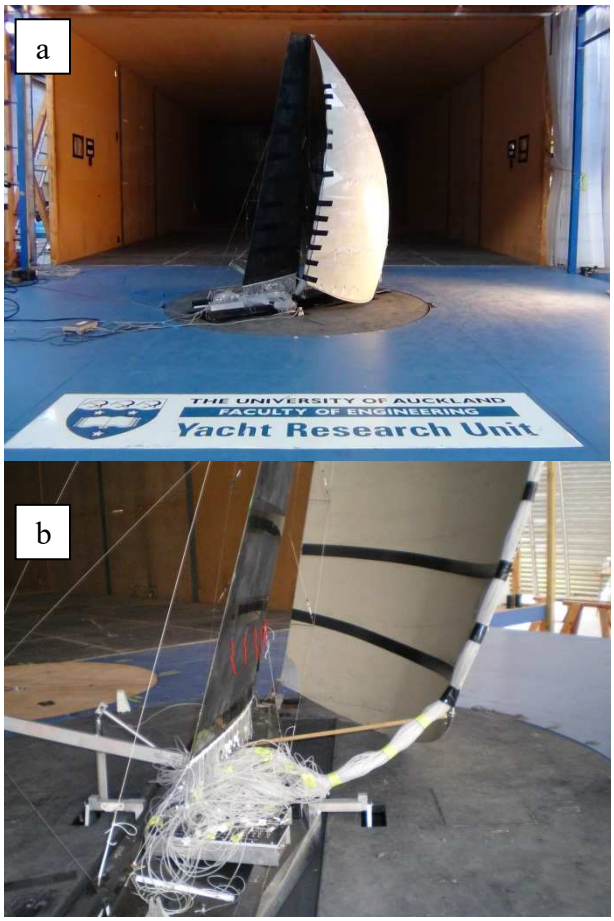

Figure 1: Photographs of the rigid spinnaker setup in the wind tunnel; (a) general view from downstream; (b) close-up view from behind the yacht model.

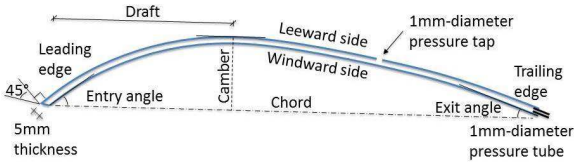

Figure 2: Sketch of a pressure tap in section of the solid spinnaker model, and definition of aerodynamic profile parameters

Measurement system and experimental procedure

All transducers were pneumatically connected to a reference static pressure measured with a Pitot-static probe located 10m upstream of the model, 0.5m below the wind tunnel roof. A total of 175 pressure taps were arranged along five horizontal sections located at fractions 1/8, 1/4, 1/2, 3/4 and 7/8 of the mitre height, which is the line equidistant from the leading and trailing edges of the sail. The distance between consecutive pressure taps ranges from around 10mm near the leading edge up to around 100mm in the middle of the chord

where the pressure gradient is expected to be lower. There are from 31 to 38 taps per section.

The reference dynamic pressure q_∞ was measured by the same sensor as described in the preceding paragraph. Two other Pitot-static probes were positioned 0.8m above the wind tunnel floor (corresponding to a full scale height of 12m) to check the air speed at these locations too.

The piezoresistive pressure sensors used are Honeywell XSCL04DC transducers, and a calibration was made before each experimental run with a precision (+/-0.125 Pa) Druck-DPI 615LP pressure calibrator. The accuracy of the pressure measurements is of order 0.5 Pa.

Pressures were measured on the 175 pressure taps on each side of the sail, for different AWA and heel angles. For the mean pressure distribution, pressures were recorded over 100s at a sampling frequency of 100Hz. Only the pressure distribution on the sail's suction side is shown for clarity. On the pressure side, the pressure was observed to be nearly constant with a pressure coefficient *Cp* ranging between 0.5 and 0.8 depending on the AWA.

Table 1: Parameters of the aerodynamic profile on each section (see definition in Fig. 2)

Section	1/8	1/4	1/2	3/4	7/8
Curve [mm]	1490	1510	1380	892	525
Chord [mm]	1260	1276	1203	820	488
Twist [°]	23	27	34	37	40
Camber [mm]	350	346	277	140	73
Camber [%]	28	27	23	17	15
Draft [%]	55	56	52	50	49
Entry Angle [°]	63	63	56	48	50
Exit Angle [°]	39	40	50	47	45

3 MEAN PRESSURE DISTRIBUTIONS

Figure 3 shows the mean pressure distributions recorded on the five sections of the spinnaker for an AWA of 55° and 10° heel.

The three lower sections show similar behaviour with the following characteristics. A high suction peak at the leading edge is followed by a sharp pressure recovery with a minimum suction located around 2% of the chord length. The flow separates at the leading edge producing a strong leading edge separation bubble giving the strong suction, and the pressure recovery is associated with re-attachment. On upwind sails [14] and on flat plates [15], the maximum pressure recovery occurs just downstream of the point of reattachment. Downstream of this point, the pressure decreases again due to the sail curvature and thus the associated flow curvature, with a maximum suction at around 20%-30% of the chord length. After the pressure recovery in the region where the sail shape becomes less curved, the pressure is nearly constant in the trailing edge separated area. The high spatial resolution achieved due to the numerous pressure taps enables the very sharp gradients occurring near the leading edge to be resolved, which has not usually been possible in previously published work on sail pressure distributions. Notice that due to different chord lengths for the different sections, suction maxima at the same reduced coordinate x/c are not superimposed in reality.

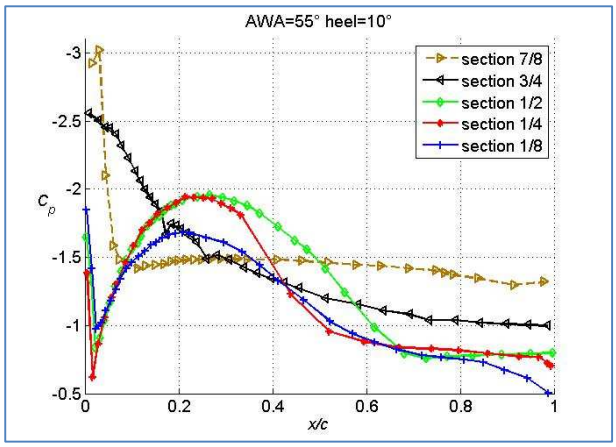

Figure 3: *Cp* on the 5 sections of the spinnaker for 55° AWA and 10° heel.

On the highest section, there is a very high suction (*Cp* = -3) at the leading edge and then a rapid pressure recovery with the minimum suction located at 10% of the chord followed by a relatively uniform pressure over the remaining chord. This pressure distribution suggests that there is a tight leading edge separation bubble (or vortex) at this location. Note that since this section is near the head of the sail, the flow will be very three-dimensional. There is a very flat maximum suction visible around x/c=0.3-0.4. On section 3/4, downstream of the high suction at the leading edge, the pressure recovery is smooth and essentially monotonic.

The pressure distributions on the five sections are shown in Figure 4 for AWAs from 51° to 59°. It should be noted that the rigid spinnaker shape corresponds (approximately) to the flying shape of the equivalent soft sail recorded at 55° AWA. This frozen shape is expected to perform well over a fairly narrow range of AWAs. Again, the three lower sections show similar behaviour to that described above. When the AWA is increased, the pressure recovery at the re-attachment location is reduced a little and the trailing edge separation point moves upstream. The pressure distribution on the lowest section is the least sensitive to AWA, whereas conversely, the pressure distribution on the highest section is the most sensitive to AWA. It may also be noticed that the pressure plateau in the trailing edge separated area for section 1/8 is more pronounced and with a higher suction (*Cp* around -0.8) for the highest AWA. The higher sections are mostly separated and totally stalled for the highest AWA.

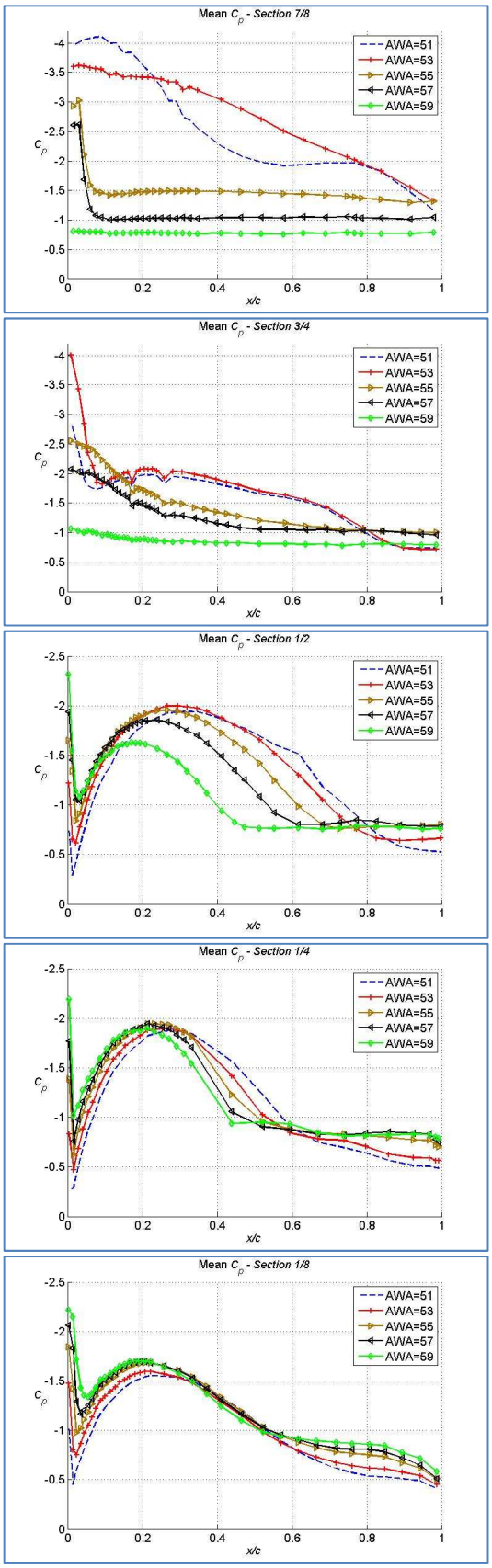

Figure 4: *Cp* for AWA=51, 53, 55, 57 and 59° on the 5 sail sections. Note that the *Cp* scale is larger for sections 3/4 and 7/8.

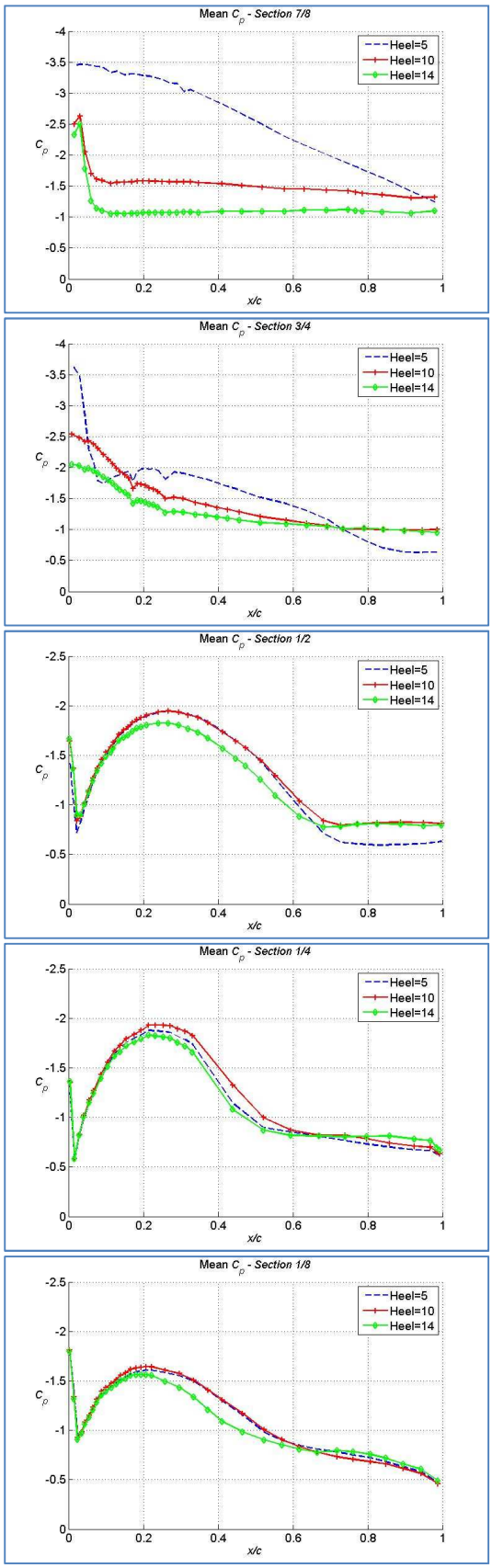

Figure 5: *Cp* for heel=5, 10 and 14° on the 5 sail sections, for AWA=55°. Note that the *Cp* scale is larger for sections 3/4 and 7/8.

Figure 5 shows the pressure distributions on the five sections for heel angles of 5°, 10° and 14°, for an AWA of 55°. On the three lower sections, the pressure is affected only slightly by heel angle, with the trailing edge separation slightly earlier for the highest heel angle. On the top two sections, where the flow is mainly separated, the effect of heel is stronger and the higher the heel angle, the more stalled the profile. In Figure 6, it is noticeable that the pressures on the top two sections at 5° heel for 55° AWA are nearly identical to pressures at 10° heel for 53°AWA, and that the pressures at 10° heel for 57° AWA are nearly identical to pressures at14° heel for 55° AWA, so that aerodynamically, additional heeling corresponds to increasing the angle of attack. In particular, the trailing edge separation point seems to move upstream when the heel angle increases.

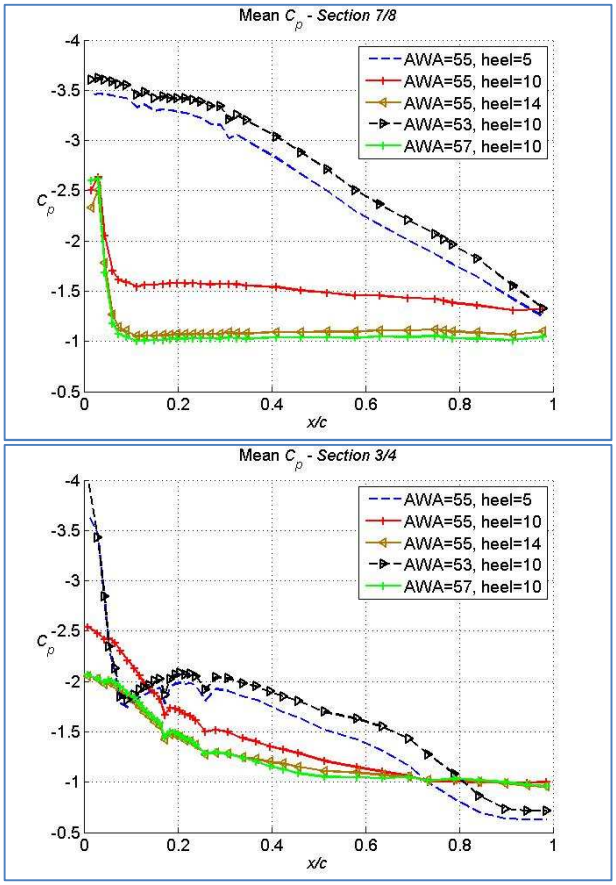

Figure 6 : *Cp* on sections 7/8 and 3/4 for AWA=55° and heel angles of 5, 10 and 14°, and for heel angle = 10° and AWAs of 53, 55 and 57°.

4 COMPARISON WITH OTHER PUBLICATIONS

Figure 7 shows the present results and those achieved with recent numerical simulations made on the same geometry at 55° AWA using Delayed Detached Eddy Simulation [16], and those achieved experimentally on the equivalent soft sail [12]. Also shown on the figure are results of the present study obtained during another

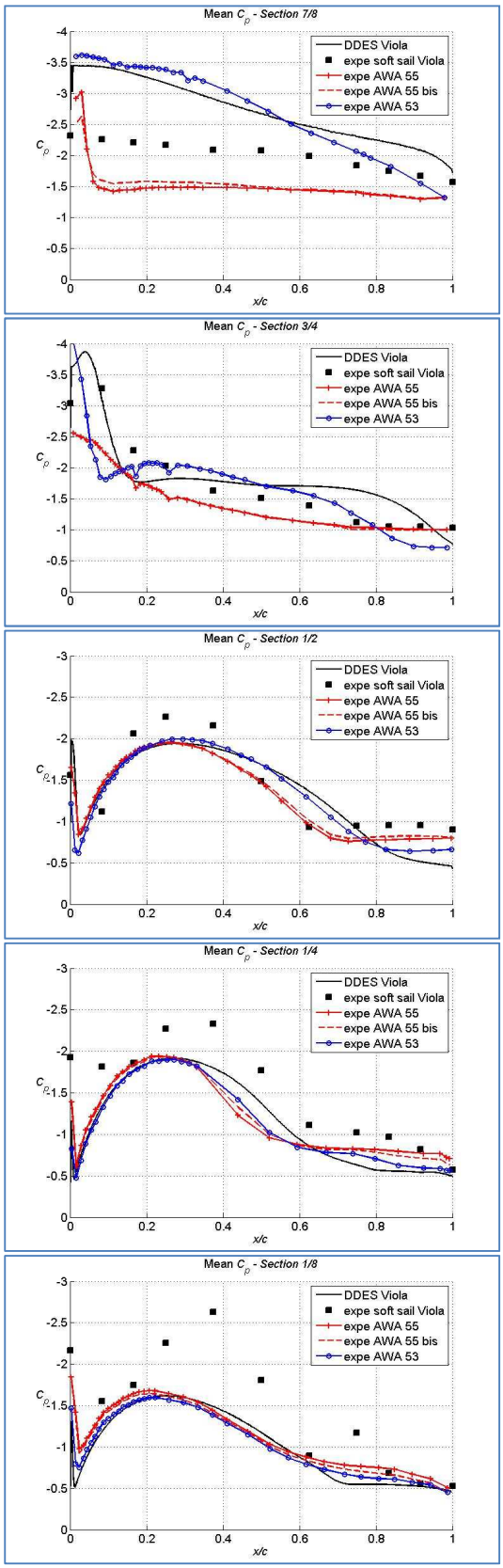

Figure 7: *Cp* measured on the solid spinnaker (present study) for AWA=53 and 55° (measurements from two distinct experimental runs are shown to assess the repeatability), measured on a soft sail [12] and computed with DDES [16].

experimental run, which show the reasonable repeatability of the measurements. On the three lowest sections, the simulated and experimental results are similar. The general behaviour is well reproduced and a good quantitative agreement is found. In some cases, the simulation result is closer to the pressure recorded for a slightly lower AWA of 53° (see sections 1/8 and 1/4 for x/c<0.2 and section 1/2 for x/c<0.4). The pressure plateau associated with the trailing edge separation is found to be a little further downstream in the simulation than in the experiment. On the top two sections, the numerical pressures are similar to the experimental result for a lower AWA (53°).

The results obtained on the soft sail in a different experiment show general behaviour that is more or less compatible with the present results, but the discrepancies are important. In particular, the peak suction values and locations are rather different. It can be observed that the lower number of pressure taps on the soft sail did not allow the sharp gradients to be resolved. The differences between the soft and rigid sail results are also likely to be due to the differences in shape between them. In fact they are also slightly different in size.

Another reason for the differences observed between the present results and the simulation results may result from an alteration of the shape of the solid sail. As the solid sail is quite heavy (around 10kg) compared to the aerodynamic force, and not perfectly rigid, it was observed after the tests that the model's weight altered the general sail shape by dropping the clew which would have increased the sail curvature and decreased the sail twist resulting in higher angle of attack on the highest sections, which could explain the stall of the top of the sail. In order to understand this point better, a subsequent research project is underway to measure both the spinnaker and mainsail pressures, with additional support of the solid spinnaker using wires to fix the distances between the head, tack and clew to the required values.

5 PRESSURE TIME SERIES

For the particular analysis of pressure time histories, some tests were done with only 58 pressure taps located on sections 1/4, 1/2 and 3/4, and with shorter pressure tubes, recorded over 300s at a sampling frequency of 200Hz. The signals were then filtered with a moving average of span 20 data points to reduce the frequency to 20 Hz. Each tube length was adjusted to the length of each flute inside the sandwich sail in order to have an identical total cavity length equal to 2.15m. Such long tubes would have provided significant damping to the recorded pressure time histories. However, even though the sensor plus tube transfer function is not known with precision, the recorded pressures show quite different behaviours depending on their positions, and hence according to the region of the local flow, and some interesting features of the separation were detected.

Figure 8 shows the time series of *Cp* variations (instantaneous *Cp* – time averaged *Cp*) on section 1/2 from four characteristic locations along the chord: near the leading edge just downstream of the reattachment (x/c=0.0428), near the maximum of the curvature suction peak (x/c=0.240), in the separation region (x/c=0.617) and in the separated area near the trailing edge (x/c=0.889). In the two first locations, the fluctuation results from the turbulence of the flow. It is noticeable that the pressure amplitudes are much higher in the separated area and that the maximum amplitudes are observed where the separation occurs. The separation location is known to be oscillatory in time and the back and forth motion of the separation point associated with its high pressure gradient gives rise to these high pressure fluctuations. Moreover, as can be seen in the enlargement in Figure 8, the pressure fluctuations at x/c=0.617 undergo rather coherent oscillations at a frequency significantly lower than the pressure fluctuations at other locations. This low frequency ranges between 0.3Hz to 1Hz, which corresponds to a Strouhal number range $St = 0.1 - 0.35$. Such a Strouhal number range suggests that these fluctuations are associated with the large scale vortex shedding in the flow separation.

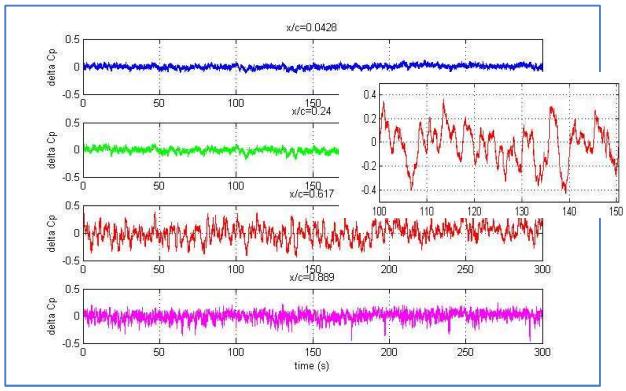

Figure 8: Time series of the *Cp* variations on section 1/2, at x/c=0.0428, 0.240, 0.617 and 0.889, enlargement: detail for x/c=0.617 and *t* from 100 to 150s.

6 DISCUSSION AND CONCLUSIONS

The paper presents results from novel rigid sails, manufactured in a sandwich structure made of pressure-tight flutes, which allows the pressure distributions on model-scale yacht sails to be measured. This model was used to measure the pressure distributions on an asymmetric spinnaker at different AWA and heel angles, and the results were compared with numerical results and another experimental method.

The measurements confirmed the general pressure distributions and trends observed by other authors with flexible sails [10,12] and numerical simulations [16]. In particular, in the optimum trim condition, the pressure gently decreases from the leading edge to the trailing edge on the whole windward side of the sail. On the

leeward side (Figure 3), the pressure shows a suction peak due to the leading edge separation followed by a partial pressure recovery associated with the turbulent reattachment. Further downstream the pressure shows a second smoother suction peak associated with the sail and flow curvature, and then a pressure plateau extended to the trailing edge when separation occurs. On the highest sections, the second suction peak does not occur due to the tip vortex at the head of the sail.

When the AWA increases (Figure 4), the leading edge suction peak increases while the trailing edge separation point moves upstream leading to a lower curvature-related suction peak. When the AWA is increased further, the flow fails to reattach and the pressure gradient decreases until a constant pressure is measured on the entire sail section.

Increasing the heel angle has a similar effect to increasing the AWA (Fig. 6). This is expected to happen only in a limited range of heel angles, such as those measured in the present paper. In fact, it was noted by several authors (for instance Le Pelley et al. [2]) that downwind sails may allow larger aerodynamic forces when the yacht is slightly heeled than when upright. However, when the heel angle increases, the effective angle of attack AWA_{eff} in a plane perpendicular to the mast decreases according to Equation (1).

$$AWA_{eff} = tan^{-1}[\tan(AWA)\cos(heel)] \quad (1)$$

Therefore, it is expected that heeling the yacht to high angles would modify the pressure distribution in a similar fashion to when the AWA decreases. Conversely, for low angles of heel, the reduction of AWA_{eff} with the heel is small. For instance, if the heel angle increases from 5° to 10°, and from 10° to 14°, AWA_{eff} decreases by 0.3° and 0.4°, respectively. Therefore, in the tested range of heel angles (5°-14°), the AWA_{eff} reduction is negligible while other phenomena, which remain to be understood, may prevail. The effect of heel on the aerodynamic force produced by a spinnaker will also depend on whether or not it is re-trimmed.

This novel model sail pressure investigation allowed progress beyond the current state-of-the-art method based on flexible sails [10,11,12] in several areas. In particular:

- Rigid sails allow better control of the sail geometry (particularly camber and draft) than flexible sails, though the control on the twist of the sails is still unsatisfactory. For instance, the comparison with the pressures computed numerically by Viola et al. [16] suggests that the sail was under-twisted by about 2° on the highest sections during the experiments (Fig. 7). This undesirable sail deflection was probably caused by its own weight.
- On flexible sails the pressure tubes cannot be bundled together at the trailing edge and thus the tubes have a greater blockage effect than with rigid sails. For instance, when pressures on the leeward side are measured with flexible sails, the tubes on the windward side deflect the incoming streamlines, resulting in an increased angle of attack. This can be seen in Fig. 7, where higher suction peaks were measured with flexible sails than with rigid sails.
- On flexible sails, the weight of the pressure taps and tubes affect the sail shape leading to local flow accelerations and pressure changes, while rigid sails allow a much smoother surface. For instance, on the lowest section in Fig. 7, the pressure around 3/4th of the chord decreases locally due to a kink (wrinkle) on the sail.

Rigid sails also allow the pressure transducers to be placed very close to the pressure tap, minimising the displacement of the volume of air between the tap and the transducer that affects the frequency content of the pressure time series due to the filtering effect of long tubes. The study of frequencies and phases of the pressure time series may reveal very interesting information on the flow field. For instance, it may allow the detection of the location of laminar to turbulent transition, if the positions of separation and reattachment points are stationary, while correlations between signals from taps located in different places may allow the convection of coherent flow structures to be detected. The paper presents a preliminary attempt to analyse pressure time histories at four different locations (Fig. 8). For the first time it is shown that the position of the trailing edge separation point is not steady but oscillates with a frequency corresponding to $St = 0.1 - 0.35$. Future work in this area is expected to include the use of shorter pressure tubes, or pressure transducers embedded into the sail structure, as is commonly done in experimental aeronautical research investigations.

In conclusion, the novel experimental methods discussed in the paper are very promising although further enhancements are needed to increase their accuracy. Firstly, the flying shape must be controlled more precisely and, secondly, it is desirable that the blockage due to the bundle of tubes at the trailing edge is decreased further.

ACKNOWLEDGEMENTS

The authors warmly acknowledge the help from the Centre for Advanced Composite Materials (CACM) at The University of Auckland to build the solid spinnaker model. The support from the YRU and especially David Le Pelley is gratefully acknowledged, as well as the help from research students Dario Motta, Francesca Tagliaferri and Novella Saccenti to carry out the tests. This research has been performed within the SAILING FLUIDS project, which is funded by the European Commission under the 7th Framework Programme

through the Marie Curie Actions, People, International Research Staff Exchange Scheme.

REFERENCES

[1] Richards, P.J., Johnson, A. and Stanton A., 2001, America's Cup downwind sails - vertical wings or horizontal parachutes?, *Journal of Wind Engineering and Industrial Aerodynamics*, Vol. 89, Issues 14–15, pp 1565-1577.

[2] Le Pelley, D.J., Ekblom, P., Flay, R.G.J., 2002, Wind tunnel testing of downwind sails, In *Proceedings of the 1st High Performance Yacht Design Conference,* pp. 155-161, Auckland, New Zealand.

[3] Fossati, F., Muggiasca, S., Viola, I.M. and Zasso, A., 2006, Wind tunnel techniques for investigation and optimization of sailing yachts aerodynamics, In *Proceedings of the 2nd High Performance Yacht Design Conference*, Auckland, New Zealand.

[4] Hansen, H., Richards, P.J. and Jackson, P.S., 2006, An investigation of aerodynamic force modelling for yacht sails using wind tunnel techniques, In *Proceedings* of the *2nd High Performance Yacht Design Conference,* Auckland, New Zealand.

[5] Fossati, F., Muggiasca, S. and Viola, I.M., 2006, An investigation of aerodynamic force modelling for IMS Rule using wind tunnel techniques, In *Proceedings of the 19th International HISWA Symposium on Yacht Design and Yacht Construction,* Amsterdam, The Netherlands.

[6] Flay, R.G.J., Jackson, P.S., 1992, Flow simulations for wind-tunnel studies of sail aerodynamics. *Journal of Wind Engineering and Industrial Aerodynamics,* Vol. 44, Issues 1–3, pp.2703–2714.

[7] Flay R.G.J., 1996, A twisted flow wind tunnel for testing yacht sails, *Journal of Wind Engineering and Industrial Aerodynamics,* Volume 63, Number 1, pp. 171-182.

[8] Le Pelley, D.J., Benzie, D., Flay, R.G.J., 2001, Correct simulation of the profiles of apparent wind speed and twist for testing yacht sails, In *Proceedings of the 9th Australasian Wind Engineering Workshop (AWES).* Townsville, Australia.

[9] Richard, P., Lasher, W., 2008, Wind Tunnel and CFD Modelling of Pressures on Downwind Sails, In *Proceedings of Bluff Bodies Aerodynamics & Applications, Milano, Italy.*

[10] Viola, I.M., Flay, R.G.J. (2009). Force and pressure investigation of modern asymmetric spinnakers, *Transactions of the Royal Institution of Naval Architects Part B: International Journal of Small Craft Technology*, *151*(2), 31-40.

[11] Viola, I.M., Flay, R.G.J., 2011, Sail pressures from full-scale, wind-tunnel and numerical investigations, *Ocean Engineering*, *38*(16), 1733-1743.

[12] Viola, I.M., Flay, R.G.J., 2010, Pressure distribution on modern asymmetric spinnakers, *Transactions of the Royal Institution of Naval Architects Part B: International Journal of Small Craft Technology*, *1512*(1), 41-50.

[13] Brett, J.S, 2012, Downwind Sail Aerodynamics: A pressure distribution and an Aerodynamic Forces database for the validation of numerical code, *Master Research in Naval Environment, Research Institute of the Naval Academy, IRENav, Arts et Métiers ParisTech, France.* Research project undertaken at the Yacht Research Unit, University of Auckland.

[14] Viola, I.M., Bot, P., Riotte, M., 2013, Upwind Sail Aerodynamics: a RANS Numerical Investigation Validated with Wind Tunnel Pressure Measurements, *International Journal of Heat and Fluid Flow,* Vol. 39, pp.90-101, DOI: 10.1016/j.ijheatfluidflow.2012.10.004.

[15] Crompton, M.J., Barret, R.V., 2000, Investigation of the separation bubble formed behind the sharp leading edge of a flat plate at incidence. In *Proceedings of the Institution of Mechanical Engineers, Part G: Journal of Aerospace Engineering*, 214(3), 157-176.

[16] Viola, I.M., Bartesaghi, S, Van-Renterghem, T., Ponzini, R., 2013, Delayed Detached Eddy Simulation of sailing yacht sails. In *Proceedings of the 3rd International Conference on Innovation in High Performance Sailing Yachts, INNOV'SAIL*, Lorient, France (present volume).

AUTHORS BIOGRAPHY

Patrick Bot, PhD, is associate Professor of Fluid Mechanics at the Naval Academy Research Institute in fluid mechanics and energy engineering. His research interests include yacht dynamics, sail aerodynamics and fluid structure interaction. His previous experience includes hydrodynamic instabilities and transition to turbulence.

Ignazio Maria Viola, PhD, is Lecturer in Naval Architecture at the School of Marine Science and Technology of Newcastle University, UK. He has a background in applied fluid dynamics and a specialist expertise in yacht engineering. His previous experience includes a Post Doctoral Fellowship at the Yacht Research Unit (University of Auckland), which formerly was the Scientific Advisor of the America's Cup team Emirates Team New Zealand, and a PhD (Politecnico di Milano) on experimental and numerical modelling of the aerodynamics of sailing yachts, sponsored by the America's Cup team Luna Rossa. Ignazio is Coordinator of the SAILING FLUIDS project.

Richard G.J. Flay, PhD, is Professor of Mechanical Engineering and Director of the Yacht Research Unit in the Department of Mechanical Engineering at the University of Auckland. He has had a longstanding research interest in the wind and sailing. His PhD degree was awarded for a study of wind structure using field measurements. His Postdoctoral research as a National Research Council Visiting Fellow in Canada was focused on wind tunnel studies in a boundary layer wind tunnel. He then spent four years as an Aerodynamic Design Engineer in an Engineering Consultancy in Toronto where he worked on the design of several wind tunnels and environmental test facilities. Since 1984 he has worked at the University of Auckland, and in 1994 he designed the World's first Twisted Flow Wind Tunnel. He has been a member of the YRU since its inception in 1987.